Journal of Aeronautics, Astronautics and Aviation, Vol. 56, No. 1S, pp. 501 – 511 (2024)
DOI: https://doi.org/10.6125/JoAAA.202403_56(1S).37

Design of a Robotic Arm for Inspecting Curved Surface in Aerospace Non-Destructive Testing

Mohd Afiq Azizi Ajman and Ermira Junita Abdullah *

Department of Aerospace Engineering, Faculty of Engineering, Universiti Putra Malaysia, 43400 Serdang, Selangor, Malaysia

ABSTRACT

The aerospace industry's reliance on inspections for component safety and readiness prompts challenges in non-destructive testing (NDT), particularly on contoured surfaces. Conventional methods, such as ultrasonic and eddy current testing, require constant probe contact which leads to slow inspections and accuracy concerns. Additionally, technicians face risks during elevated point inspections, necessitating a safer and efficient solution. To address these challenges, this study proposes a specialized robotic arm for NDT inspections in aerospace. The robotic arm automates inspections, enhancing efficiency, accuracy, and technician safety. The research aims to validate the robotic arm's performance, certifying its capability for NDT inspections on curved surfaces which ushers in a new era of enhanced practices. Using CATIA software, the project progresses through preliminary, conceptual, and detailed design stages. The fabricated robotic arm integrates with a trajectory planning and feedback system, enabling curved surface scanning while maintaining a normal probe trajectory. The system yields a 4.3 percent of error emphasizing the system's precision, with rigorous testing using myRIO and infrared (IR) sensor confirming the robotic arm's ability to maintain a 2-mm distance from the scanned surface. This validates the system's efficacy and its capacity to autonomously uphold a specified distance during scanning. This innovative robotic arm and control system significantly impact aviation NDT, improving inspection practices, safety, and industry standards. The study not only validates the robotic arm's effectiveness but also sets the stage for future innovations in robotic NDT, benefiting sectors reliant on quality control and safety. The dual emphasis on precision and safety underscores the transformative potential of this research.

Keywords: Curved surface, Robotic arm, Control system, Normal trajectory, Non-destructive testing

I. INTRODUCTION

Safety is always the paramount issue in aviation. All flying aircraft will have to go through periodic scheduled maintenance checks and inspections to ensure that they are safe to fly [1]. Curved structures that are commonly found in aircraft components like wheel, pipes, pressure vessels and corner pieces pose a significant safety and reliability challenge due to stress concentration [2]. In conjunction to this, a robust and accurate non-destructive testing (NDT) method is vital for identifying flaws in such structures. To date, the main applications of NDT in the aerospace fields also include to detect crack, evaluate fracture propagation, identify the signs of potential stress or fatigue failures and monitor corrosion development, which are crucial for both in-service aircraft inspections and material or component manufacturing [3,4]. Currently, manual ultrasonic testing (UT) dominates the industry, yielding variable outcomes as it is highly dependent on the operator's skill. Scanning large surfaces with small UT transducers is time-

Manuscript received, November 18, 2023, final revision, January 7, 2024
* To whom correspondence should be addressed, E-mail: ermira@upm.edu.my

consuming and also labor-intensive. Moreover, the expert evaluation of inspection results further extends the process and might also compromise accuracy [5]. To address these challenges, more efficient and effective UT inspection process through the integration of robotic arms has been of high interest. These autonomous and precise instruments hold a great promise in elevating inspection practices [6].

Robotic arms that are resembling the human arm have gained traction across different industries for their offered benefits, which include 24/7 operation, reduced cycle time, enhanced industrial flexibility, improved product quality and much safer working environment [7]. The aerospace industry, being at the forefront of automation innovation, acknowledges the vast potential of the industrial robots in cutting operational costs, especially in terms of high-value manufacturing with significant order backlogs. Embracing robotic applications in aircraft engine assembly, drilling, and painting airframes, aerospace industry has capitalized on their dependability, capability and precision [8]. For automotive manufacturing, these arms ensure precision and speed in tasks like welding and assembly, while in civil engineering they facilitate tasks such as construction, inspection of critical structures, and maintenance, enhancing efficiency and safety in both industries. In fact, by collaborating with humans, these robots can take over many dangerous, tedious and repetitive tasks

In the ever-evolving landscape of NDT, the quest for enhanced productivity, better safety and more integrated data acquisition systems has driven the industry forward [9]. However, the traditional UT inspection face intriguing challenges that demand new innovative solutions. There are certain issues that are commonly seen in the process. First of all, UT are often labor-intensive and time-consuming. Manual inspections need skilled NDT technicians to scan components, which can be physically demanding and lack automation. For the complex structures, achieving consistent results becomes difficult and large samples may take hours to inspect due to small UT probe [10]. To improve efficiency and reduce operational costs, there is a need to decrease the inspection time in the aerospace industry. On the other hand, false calls in UT occur when the inspection process incorrectly identifies a defect that is not actually present. This situation could happen when the probe moves too quickly or doesn't make sufficient contact with the surface, leading to incorrect detections. Manual inspections often result in making false calls, necessitating repeated inspections to ensure the accuracy of the findings [11]. Based on a recent study, a comparison between manual and automated eddy-current testing (ECT) shows that manual inspections tend to have more false calls [12].

Within the expansive sectors of aerospace and automotive industries, robotic arms have demonstrated exceptional proficiency in tasks such as welding, trimming, picking, and positioning. These capabilities find application across a diverse range of tasks and industries. In general, these tasks are classified based on geometrical characteristics, kinematic structure, applications, actuating joint methods and intelligence, including a method being based on their "work envelope" that will define their reach and interaction area. In the aerospace industry, the robotic arms have been used for repetitive tasks like picking and placing items along assembly lines. Path planning methods that are employed in these operations include the trajectory planning and the real-time control. The trajectory planning involves manual teaching, where the robot learns and also stores path points for later repetitive tasks. For inspecting curved surfaces, the robot's capability to learn the specific configurations is crucial [13]. This enhances accurate and repeatable movements during real-time control, especially when dealing with the unpredictable tasks aided by sensors like cameras. The coordination of the robot's movements distinguishes between the trajectory planning and the real-time control, making the manual teaching as an essential component. The recorded joint values serve as a reference for subsequent movements, ensuring the precision and the reliability required for the aerospace UT inspections of curved surfaces.

With the aim of revolutionizing NDT inspections in aerospace industry, the research work done delves into the transformative potential of robotic arms. This study seeks to enhance the robotics arm application, especially in UT inspection. The automated inspection on curved surface have been pioneered by [3]. However, there are certain limitations that need to be addressed, such as the robotic arm not possessing the capability for intuitive and adaptive interaction with the inspection environment. The paper proposes a fully automated robotic arm driven by Arduino and NI myRIO, equipped with various sensors for a seamless inspection process. By emphasizing on the feasibility of robotic arms in conducting automated UT inspections, this research marks a crucial step towards the advancement of inspection practices, boosting safety and elevating the aerospace industry into an era of cutting-edge technology.

II. SETUP AND METHODOLOGY

For the design of a robotic arm for inspecting curved surfaces, these versatile machines play a crucial role. Their tasks include data gathering and also hazardous location research, reducing human interference by almost 50% [14]. The main objective for this research is to develop the control system for a robotic arm that is capable to scan a contoured surface. This process involves the initial design process from the robotic arm structure to the integration of the control system. The system of the robotic arm has been programmed using Arduino and myRIO. Also, the robotic arm has two control system for data measurement and also its motion. The motion of the robotic arm is done using a trajectory planning method in which the motion is being recorded and executed during scanning process. After the robotic arm is able to function, the data measured by the sensor can visualize its performance to maintain a normal trajectory to a contoured surface. The overall flowchart of methodology for this research study is shown in Figure 1.

The robotic arm was design using the engineering design process which contained requirements, conceptual, preliminary, and detailed design. As for the design requirements, it is influenced by the required work envelope which represent the volume their end effector

could reach. This envelope is determined by three main characteristics: the range of robot joints, size of the robot body and wrist, and type of joints used. Based on [15], Cartesian robots are widely used in the aeronautical sector because it is easy to know the position of the transducer in the piece at each moment. However, every time the pieces to be inspected are more complex, and it is not possible to use Cartesian robots; therefore, complex industrial robots must be used. In this study, the aim is to design a robotic arm that maintains a normal trajectory on contoured surfaces like aircraft components. To accomplish this, the end effector must move in angular positions up to 180 degrees, necessitating combined rotary joints for a spherical work envelope. This design ensures effective maintenance of a normal trajectory on contoured surfaces. The robot's mobility is described by degrees of freedom (DOF) and a 5-DOF robotic arm is proposed for moderate mobility. The end effector's sensor board, shown in Figure 2, requires a normal trajectory to the cylinder's surface while maintaining a distance during the scanning. To allow for this, the robotic arm's end effector must have at least 3-DOF in the (x, y, z) coordinates, with Joint-4 orienting the sensor board parallel to the surface. Joint-5 adjusts the sensor board's angle to keep Link-5 normal to the surface during scanning. In this study, the test object is a scaled-down Airbus A320 wheel tire prototype, 30% of the original size.

After the design requirement is being identified, the conceptual design is being done using the morphological matrix approach. Firstly, the conceptual design begins by gathering the inputs for various option of the robotic arm. These inputs encompass user demands, technological requirements and also financial restrictions, among others, defining scope and limitations of the study as shown in Table 1. Based on these options, three design concepts have been derived to be further analyzed in this study. The three design concepts are tabulated in Table 2.

Based on the designs created using the morphological matrix approach, the evaluation whether the design is meeting the requirement is presented using Pugh matrix approach. The conceptual design will be scored based on several criteria. It should be noted that the score is made based on a simple Likert scale between 1 to 9, whereby 1 is very poor while 9 is assigned for outstanding evaluation. Table 3 presents the results for the evaluation of the three considered design concepts. As can be observed, there are six evaluation criteria that have been considered for these robotic arm design concepts. A large working envelope is crucial for versatile movement, while a high movement efficiency is essential for scanning curved surfaces. Other considerations include good reflex for hand gesture replication, stable data during scanning, easy programming with fewer joints, quick fabrication for time management and high material availability for replacements. Based on Table 3, Design 1 is shown to have received the highest score and it has been selected as the robotic arm design for this study.

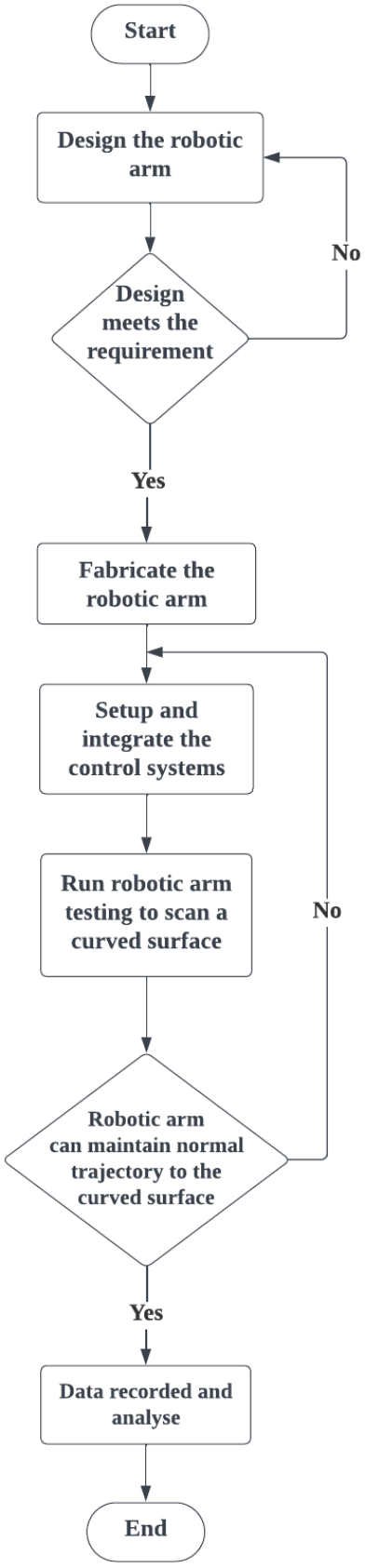

Figure 1 Methodology flowchart for this study

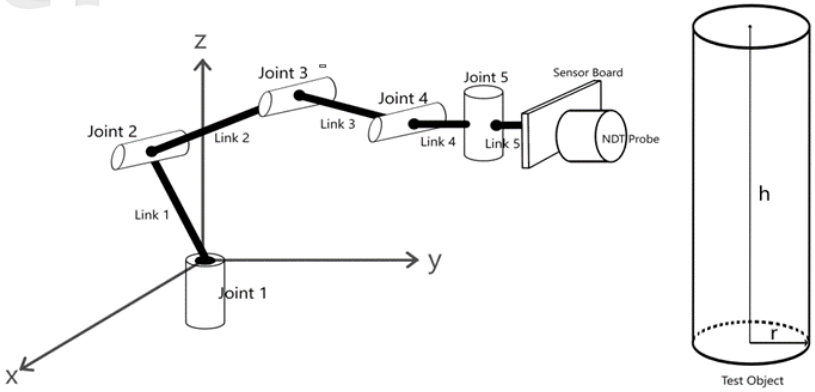

Figure 2 Robotic arm concept

Table 1 The inputs for the robotic arm design concept

Input	Option 1	Option 2	Option 3	Option 4	Option 5
Type of robotic arm	Articulated	SCARA	Cartesian	Delta	Cylindrical
Degree-of-freedom	3	4	5	6	7
Type of joint	Revolute	Prismatic	Planar	Universal	Cylindrical
Material	Plastic	Metal	Aluminium	Glass Fibre	Wood
Base shape	Circle	Rectangle	Square	Hexagon	Pentagon
Size	Small	Medium	Large		
Cost	Low	High			

Table 2 Considered alternative concept designs for the robotic arm

Element	Design 1	Design 2	Design3
Type of robotic arm	Articulated	SCARA	Delta
Degree of freedom	5	3	7
Type of joint	Revolute	Cylindrical	Universal
Material	Aluminum	Plastic	Metal
Base Shape	Rectangle	Square	Circle
Size	Small	Large	Medium
Cost	Low	Low	High

Table 3 Pugh matrix evaluation of the robotic arm design concepts

Criteria	Weightage	Design 1		Design 2		Design 3	
		Mark	Percentage	Mark	Percentage	Mark	Percentage
Large working envelope	40%	9	40.0	5	22.2	7	31.1
High movement efficiency	25%	7	19.4	5	13.9	9	25.0
High strength and stability	15%	7	11.7	4	6.7	9	15.0
Ease of programming	10%	5	5.6	9	10.0	3	3.3
Ease of fabrication	5%	6	3.3	9	5.0	4	2.2
Easily available in the market	5%	9	5.0	8	4.4	3	1.7
Total	**100%**	**85%**		**62.2%**		**78.3%**	

Regarding the robotic arm's construction, it is assembled using anodized aluminum components readily available in the market. This structure functions as the linkage for each joint, with servos connecting them

securely through screws and nuts. Additionally, a bespoke controller, featuring five potentiometers and soldered wires, facilitates the arm's movement. To ensure safety and stability, this controller is securely housed in an enclosed casing. At the end effector of the robotic arm, a sensor board is incorporated, comprising a distance sensor and servo components. This sensor board plays a crucial role in ensuring that the end effector remains perpendicular to the curved surface during the scanning process.

A sophisticated control system is employed to manage the robotic arm's intricate movements, consisting of an Arduino microcontroller equipped with five servo motors, four potentiometers, and two Time-of-Flight (ToF) laser sensors. The joint motion strategy involves delicately approaching the scanning surface while maintaining the sensor board's parallel orientation to the surface's contours. For trajectory planning, four servos and four potentiometers play a crucial role in determining the angles for each servo, thereby establishing the precise path for the sensor board to traverse. The potentiometers govern the movement of the robotic arm's base, shoulder, elbow, and wrist. This system enables the recording and subsequent replay of motions, facilitating a comprehensive inspection of contoured surfaces. The iterative recording process ensures consistent proximity of the sensor board to the surface, guaranteeing reliable data collection. A visual representation of the robotic arm's motion workflow is depicted in Figure 3 for clarity and reference.

Figure 3 Flowchart for robotic arm motion

The system will maintain the normal trajectory using laser sensors. It has been proposed to use three distance sensors as depicted in Figure 4.

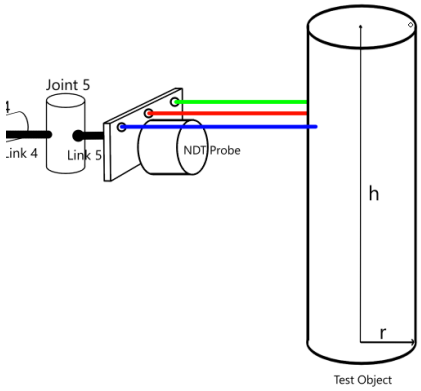

Figure 4 Setup of the sensors

Based on the figure, two distance sensors are used to adjust the angle of the sensor board, which are Sensor 1 (Green) and Sensor 2 (Blue). In the meantime, the other sensor is used to measure a certain distance from a surface, which is Sensor 3 (Red). As for that, three type of distance sensors: Ultrasonic, Sharp Infrared (IR) and ToF laser are considered for affordability and accurate distance measurement capabilities.

In the process of identifying the optimal sensors for the robotic arm application, a systematic evaluation was conducted through a controlled experiment. Each sensor underwent testing, wherein it was securely positioned at a predetermined distance from the target surface. The testing protocol was programmed using Arduino to ensure precision and consistency. The experiment commenced with each sensor maintaining a fixed distance of 1 cm from the surface. Subsequently, each sensor recorded its distance readings for a standardized duration of 10 seconds. The evaluation of each sensor's ability to sustain its measured values was accomplished by generating a graphical representation, plotting the distance measured against the elapsed time. This methodological approach served to discern the sensors' performance and select the most suitable ones for the intended robotic arm application.

Next, the sensor board is equipped with a feedback system that ensures it maintains a consistent distance parallel to a contoured surface. The primary goal is to ensure that both sensors measure a similar distance. A visual representation of the feedback system can be found in Figure 5, depicted in the block diagram.

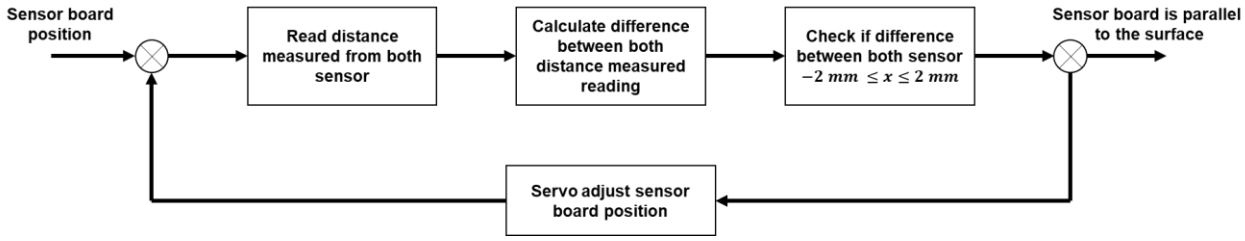

Figure 5 Feedback system for the sensor board

For this study, the feedback system's objective is to ensure that the readings from both sensors are nearly equal, with a tolerance of 2 mm. To achieve this, the position of the sensor board will be adjusted using a servo mechanism.

The servo is responsible for moving the sensor board either to the left or right side. If the calculated difference value between the sensor readings is positive, the servo will turn to the left. Conversely, if the difference value is negative, the servo will turn to the right.

The test setup for this study is the robotic arm itself and an object with a contoured surface. The setup is shown in Figure 6 and Figure 7.

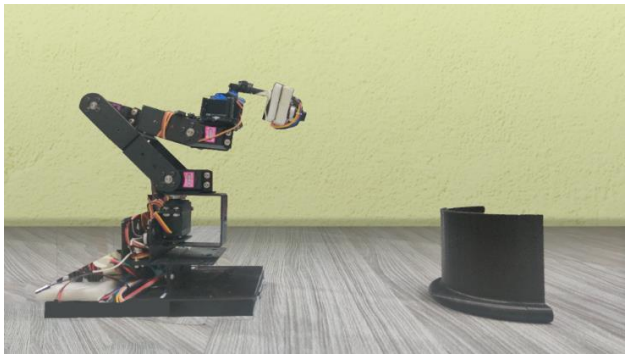

Figure 6 Side view of test setup

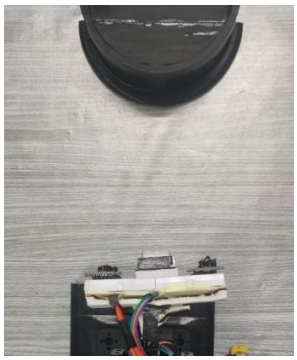

Figure 7 Top view of test setup

In this study, a scaled down Airbus A320 wheel model has been fabricated and tested. The model is shown in Figure 8.

Figure 8 Scaled down A320 wheel model for curved surface scanning test

The robotic arm performance was tested by visualizing on how it can maintain a fixed distance from the curved surface. The evaluation of the robotic arm's performance involves assessing its ability to consistently maintain a predetermined distance from a curved surface. The performance testing procedure commences with a sequence of three trials. In each trial, a pre-recorded trajectory for the robotic arm's approach to the specimen is established using the potentiometer and reset for subsequent trials. This process aims to demonstrate the efficacy of the sensor board feedback system in sustaining a fixed distance from the curved surface under varying conditions. Throughout the tests, the placement of the curved surface remains constant, and the evaluation is conducted within a single complete cycle of curved surface scanning. This controlled approach ensures a thorough examination of the robotic arm's performance in maintaining distance across different scenarios.

For data collection, the NI myRIO was connected to the middle sensor at the robotic arm sensor's board. The sensor that being use is IR sensor and it provided distance measured over time during the curved surface scanning. The IR sensor operates using two lenses which is infrared emitter and array sensor as shown in Figure 9.

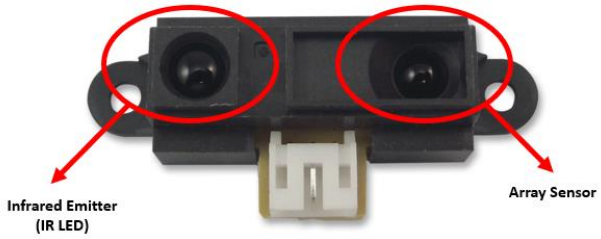

Figure 9 Sharp IR sensor

For the infrared emitter, it produces a 10 kHz modulated signal. The array sensor can detect and produce a voltage that is proportional to the position of the light incident on the signal produced.

The working principle of the IR sensor is shown in Figure 10.

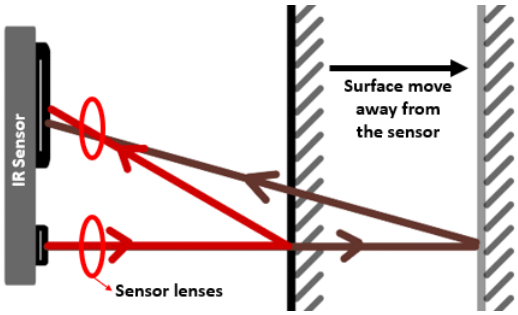

Figure 10 The signal wave reflected to the array sensor

Imagine that the sensor is place in front of a reflective surface, then the IR signal is transmitted and reflected off incident to the sensor array. Imagine that the reflective surface moves to a farther distance, the signal will bounce back and impinged to the array sensor at different position. Hence, the light spot on the array sensor indicates the

range of the reflective surface. By applying geometry on the signal pattern as shown in Figure 11, the position detected can be translated into range.

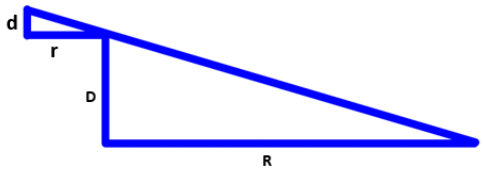

Figure 11 The geometry of the signal path

D is the range between two sensor and R is the range between the sensor and the surface. Also, d is the difference between spot of lights and r is the distance between the lens and array sensor after the reflective surface has been move farther away. Based on the sketch of the reflected signal, two identical triangles are produced. Hence, the ratio of two triangles can be used to derive an equation to convert the light position into distance measured.

$$\frac{d}{D} = \frac{r}{R} \rightarrow R = \frac{rD}{d} \quad (1)$$

Based on the derived equation of R, it can be seen that it is influenced by the denominator which is d; difference of the spot of lights at the array sensor. As the array sensor is produced voltage proportional to the position of light incident, the equation can be transformed into.

$$R = \frac{rD}{d} \times \frac{1}{v_0} \rightarrow R = \frac{K}{v_0} \quad (2)$$

Where K is a constant obtained from sensor calibration. Hence, the final equation to find the distance measured from the IR sensor is.

$$R = \frac{K}{v_0} \quad (3)$$

The equation depicted in Equation (3) is being used to measure the distance between sensor and surface using NI myRIO.

As can be seen illustrated in Figure 12, it is the program on how the IR sensor will function. The IR sensor connects to an analog input and LabVIEW's signal processing generates the signal wave, averaging every twenty data points with a sample length of 20. The voltage output estimates distance in centimeters via the conversion equation. During scanning, the waveform chart updates the measured distance continuously. After robotic arm scanning has been completed, the measurement loop will stop but the waveform graph stores data using a loop tunnel and indexing mode, creating an array for analysis. The conversion equation that is implied to the LabVIEW determines the distance between sensor and surface, d. It is calculated using Equation (1), where K is the correction factor, V is the voltage received and d_{offset} is the offset from actual distance.

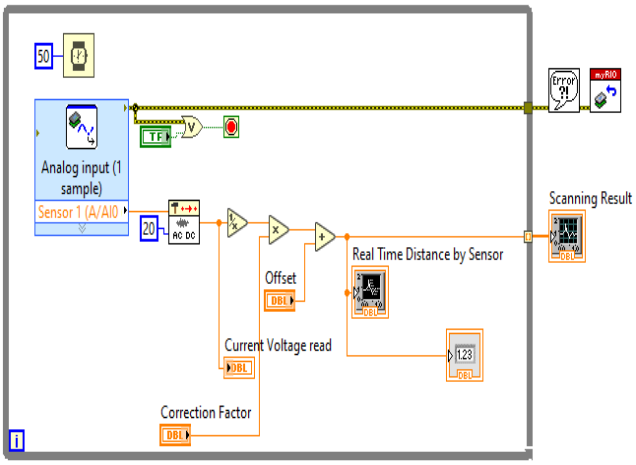

Figure 12 Graphical programing of the IR sensor operation

$$d = \frac{k}{V} + d_{offset} \quad (4)$$

III. RESULTS AND DISCUSSION

Based on Table 4, four criterias have been assessed for the sensors: consistency, weight, maximum and minimum distance, and angular dependency. The ToF Laser Sensor is chosen due to its light weight and angular dependency, which ensures the accurate distance measurement without being influenced by the surface angles. On the other hand, Table 5 comparison has revealed that TowerPro MG996R servo is the optimal choice for this robotic arm design. It meets the minimum torque requirement and is also lighter compared to other options like SPT5410.

Table 4 Comparison of distance sensor

Criteria	Ultrasonic Sensor (HC-SR04)	Sharp IR Sensor (GP2Y0A21YK0F)	ToF Laser Sensor (VL53L0X)
Consistency	Medium	Low	High
Weight	9.0 g	3.5 g	0.5 g
Minimum distance	0 cm	0 cm	2 cm
Maximum distance	80 cm	15 cm	20 cm
Angular factor	No	No	Yes

Table 5 Comparison of servo motor

Criteria	Fitec FS5109 M	TowerPro MG996R	SPT5410
Torque	Low voltage: 9 kg-cm High voltage: 10.3 kg-cm	Low voltage: 9.4 kg-cm High voltage: 11kg-cm	Low voltage: 7.6 kg-cm High voltage: 10 kg-cm
Weight	56 g	55 g	57 g

The robotic arm's structure is then constructed using the ionized aluminum parts. In this study, repeated pieces are used for easy modifications. The arm is divided into a few sections: base, shoulder, elbow, and wrist, mimicking the flexibility of a human hand. These sections are shown in Figure 13 through created computer-aided design (CAD) drawings for the robotic arm. The robotic arm is fabricated and integrated with the control system as shown in Figure 14. In the meantime, Figure 15 depicts the circuit diagram for the robotic arm.

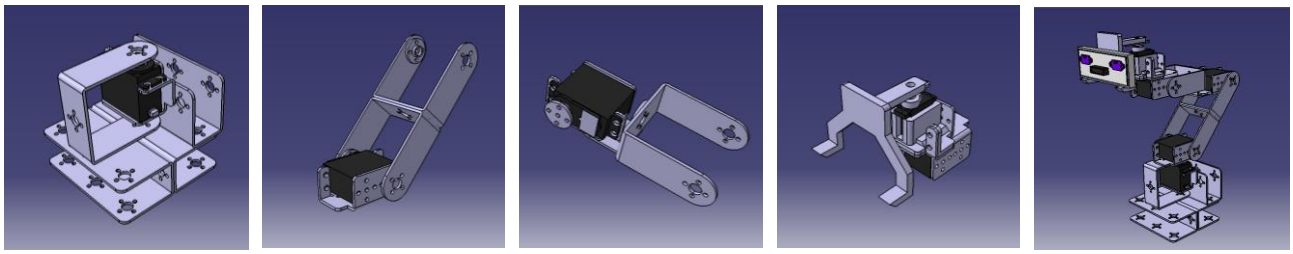

(a) Arm base (b) Arm shoulder (c) Arm elbow (d) Arm wrist (e) Overall assembly

Figure 13 CAD drawings of the robotic arm design

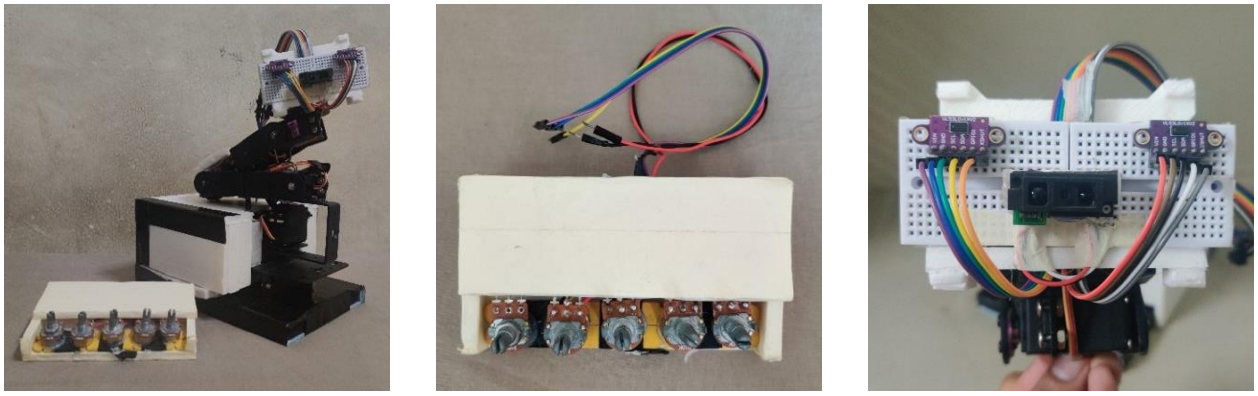

(a) Full assembly of robotic arm (b) Top view of the controller (c) Front view of sensor board

Figure 14 Resultant robotic arm that is fabricated and integrated in this study

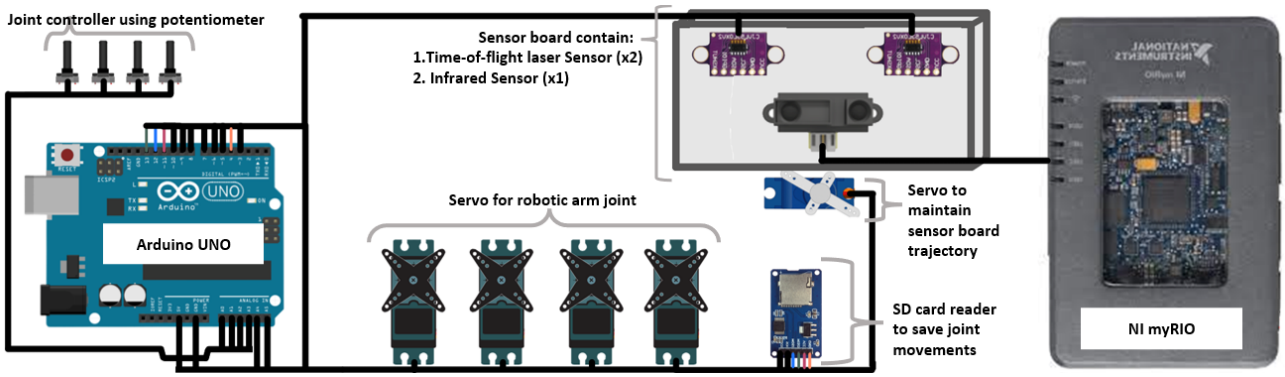

Figure 15 Circuit diagram

The performance data of the robotic arm for scanning curved surface is obtained using LabVIEW wave graph indicator. Three trials have been conducted and the results are summarized in Table 6. In addition, the plot of the distance measured by the IR sensor to the contoured surface for each trial recorded and plotted in a waveform graph. These graphs are indicating the robotic arm's ability to maintain a consistent scanning on the contoured surfaces. It also evaluates the arm's capability to align the NDT probe in parallel with the curved surface. The results are also presented for analysis.

Table 6 The results for curved scanning test using the robotic arm

Trial	Average distance measured during scanning (mm)	Response Time (s)	Percentage Error (%)
1	2.03	4.0	1.5
2	2.07	5.0	3.5
3	1.82	6.0	9.0

During the performance testing of the robot, three distinct results have been observed to assess the robotic arm's ability to consistently maintain a normal trajectory between the NDT probe and the contoured surface being scanned. An infrared (IR) sensor is employed to measure the distance between the sensor and the curved surface. For each trial, the results of the measured distance are visualized using a waveform graph; illustrating the distance over time. Recordings begin as the robotic arm approaches the curved surface and continue until the scanning process is completed. Three distinct phases are identified: A - approaching the test subject, B - scanning the test subject, and C - returning to the initial position, as depicted in Figure 16.

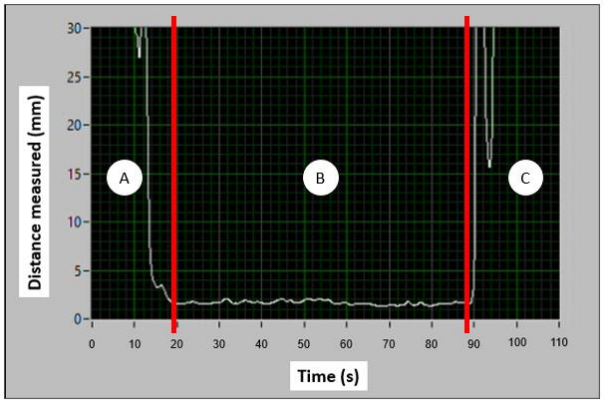

Figure 16 Phases during the distance measurement

Examining the graph (Figures 17, 18 and 19), the distance measurements are consistently recorded at 2 mm intervals starting from the 20-second time stamp until the completion of the scanning process. The study's findings indicate that the sensor successfully follows the intended path along the curve, minimizing deviations in distance while maintaining a normal trajectory. It is noteworthy that if the sensor is not positioned normal to the contoured surface, the measured distance value is not maintained emphasizing the importance of proper alignment for accurate UT inspections.

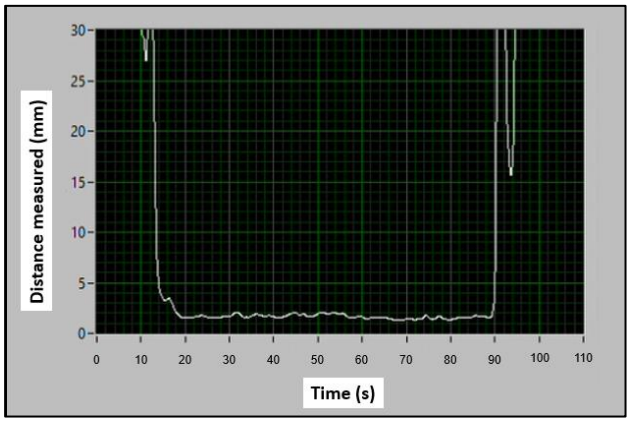

Figure 17 Distance measured in Trial 1

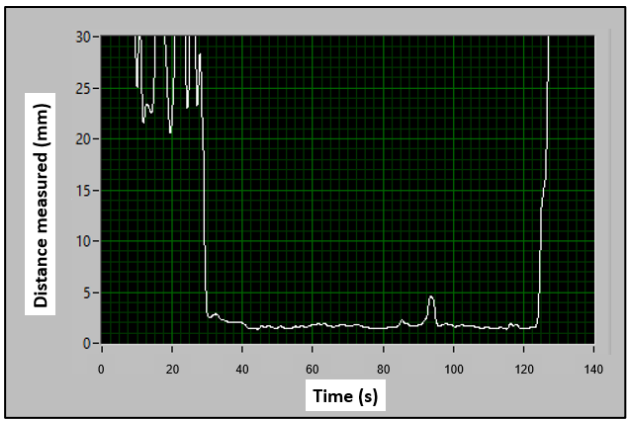

Figure 18 Distance measured in Trial 2

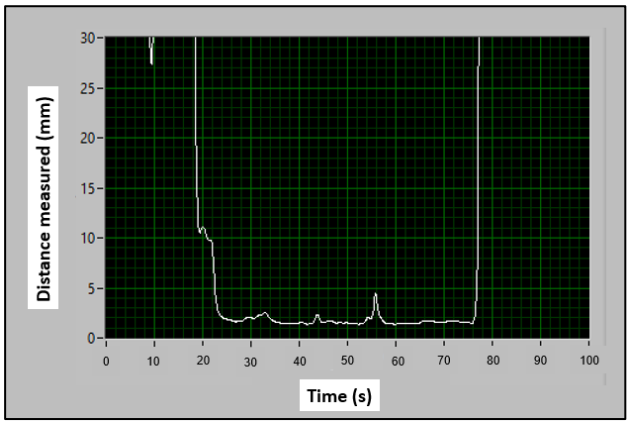

Figure 19 Distance measured in Trial 3

The system's effectiveness is analyzed based on the average distance measured during scanning, time response, and percentage error for each trial, with the system maintaining an approximate 2 mm distance from the surface. Based on Table 6, the average of the accumulated percentage error from three trials resulting a 4.3 percent of error. This shows that the system has a lower percentage error which indicates its high accuracy in inspecting curved surfaces during Aerospace Non-Destructive Testing (NDT). The design of the robotic arm incorporates advanced sensing technologies and precise control mechanisms, allowing it to navigate and adapt to the intricacies of curved surfaces with exceptional precision. This low percentage error is a testament to the efficacy of the proposed design in achieving reliable and accurate inspection results, crucial for ensuring the integrity and safety of aerospace components. The robotic arm's ability to minimize errors underscores its potential to significantly enhance the efficiency and effectiveness of NDT processes in the aerospace industry. Next, it's important to note that the term "response time" in this context refers to the system's reaction time to changes in the environment or trajectory deviations, not to be confused with the data acquisition rate. Unfortunately, the data acquisition rate is not explicitly provided in this paragraph, and it is crucial to understanding the frequency of measurements and the system's ability to respond in real-time. The observed fluctuations in the graph may be attributed to differences in the control systems of the robotic arm and sensor board, suggesting potential improvements for smoother scanning and real-time control implementation. Further details on the data acquisition rate would provide a more comprehensive understanding of the system's responsiveness.

It should be noted that few problems arose with the constructed robotic arm during this study. Vibrations have been observed from the shoulder to the sensor board in the scanning process, which can be attributed to the shoulder servo's insufficient torque that is caused by the unexpected weight increase of 23%. To address this, the rubber band damper has been added in order to reduce vibrations and improve scanning. Power supply issues have also occurred that lead to the unsynchronized movement between the potentiometer and servos. A separate power supply for the servos has resolved this problem. Despite challenges, the robotic arm's application in the aerospace brings notable benefits to safety, health and job satisfaction. To ensure the reliability and safety, rigorous testing and maintenance procedures are essential. Opportunities for improvement and customization of the robotic arm have presented vast possibilities for achieving more accurate and consistent data capture in various applications. All in all, the robotic arm's performance testing demonstrates its capability to maintain a consistent scanning trajectory and proximity to the contoured surface, highlighting the areas for potential improvement in achieving even smoother scanning results.

V. CONCLUSIONS

In conclusion, the project has successfully executed a comprehensive engineering design process to develop a robotic arm with outstanding performance. The fabricated robotic arm has been seamlessly integrated with a meticulously designed control system, showcasing remarkable advancements in trajectory planning and feedback systems. Quantitative assessments of the robotic arm's efficacy in curved surface scanning have been conducted, yielding compelling results.

The data analysis reveals that the robotic arm, employing the trajectory planning method and feedback system, demonstrates a commendable time response of 5 seconds and a consistency rate of 2 mm/s between the sensor and curved surfaces. These results significantly surpass the initial design requirement of achieving a minimum time response of 10 seconds and consistency within 5 mm tolerance. Furthermore, the system's ability to autonomously control and maintain a normal trajectory on curved surfaces has been validated. This accomplishment aligns with the design requirement of ensuring precise and stable movement during scanning operations.

Looking ahead, several enhancements can be considered for future studies of the robotic arm. Firstly, the implementation of a defect detection mechanism within the control system, utilizing myRIO and LabVIEW, is recommended. Secondly, real-time robotic arm motion using sensors and virtual coordinates should be incorporated to ensure superior synchronization compared to the current playback method. To optimize movement accuracy and torque, the adoption of NEMA 17 and A4988 stepper motors as joint actuators is advisable, addressing the design requirement of optimal joint movement. Additionally, the incorporation of a moveable robotic arm base is proposed to expand the working area while minimizing the number of degrees of freedom, as specified in the initial design requirements. In terms of power supply, transitioning to a super polymer lithium-ion battery with a voltage regulator is recommended for improved stability and performance, aligning with the design requirement of 6 volt for each servo.

In summary, the integration of the robotic arm in NDT scanning has not only met but exceeded the defined design requirements. The quantitative results attest to its exceptional scanning speed, accuracy, and autonomous trajectory control, positioning it as a leading solution in advancing industries and shaping the future of automation.

REFERENCES

[1] Shukri SA, Romli FI, Badaruddin WTFW, Mahmood AS, “Importance of English language in aviation maintenance: A Malaysia case study,” *Journal of Aeronautics, Astronautics and Aviation*, Vol. 53, No. 2, 2021, pp. 113-119.

[2] Panda RS, Rajagopal P, Balasubramaniam K, “Rapid guided wave inspection of complex stiffened composite structural components using non-contact air-coupled ultrasound,” *Composite Structures*, Vol. 206, 2018, pp. 247-260.

[3] Chen Q, Xie Y, Cao H, He Z, Wang D, Guo S, “Ultrasonic inspection of curved structures with a hemispherical-omnidirectional ultrasonic probe via linear scan SAFT imaging,” *NDT & E International*,

Vol. 129, 2022, 102650.
[4] Shahrim MA, Harmin MY, Romli FI, Ciang CC, Lee JR, "Damage visualization based on frequency shift of single-mode ultrasound-guided wavefield," *Journal of Aeronautics, Astronautics and Aviation*, Vol. 54, No. 3, 2022, pp. 297-305.
[5] Ridley SJ, Ijomah WL, Corney JR, "Improving the efficiency of remanufacture through enhanced pre-processing inspection–a comprehensive study of over 2000 engines at Caterpillar remanufacturing, UK," *Production Planning & Control*, Vol. 30, No. 4, 2019, pp. 259-270.
[6] Troughton AJ, "The value of non-destructive testing in the aircraft industry," *The Aeronautical Journal*, Vol. 71, No. 675, 1967, pp. 185-192.
[7] Almurib HA, Al-Qrimli HF, Kumar N, "A review of application industrial robotic design," Proceedings of International Conference on ICT and Knowledge Engineering, 2011.
[8] Bogue R, "The growing use of robots by the aerospace industry," *Industrial Robot: An International Journal*, Vol. 45, No. 6, 2018, pp. 705-709.
[9] Trampus P, "NDT challenges and responses-an overview," Proceedings of International Conference of the Slovenian Society for Non-Destructive Testing Application of Contemporary Non-Destructive Testing in Engineering, 2013.
[10] Towsyfyan H, Biguri A, Boardman R, Blumensath T, "Successes and challenges in non-destructive testing of aircraft composite structures," *Chinese Journal of Aeronautics*, Vol. 33, No. 3, 2020, pp. 771-791.
[11] Sattar TP, Brenner AA, "Robotic system for inspection of test objects with unknown geometry using NDT methods," *Industrial Robot: An International Journal*, Vol. 36, No. 4, 2009, pp. 340-343.
[12] Kujawińska A, Vogt K, Hamrol A, "The role of human motivation in quality inspection of production processes," Proceedings of the AHFE International Conference on Human Aspects of Advanced Manufacturing, 2016.
[13] Mineo C, Pierce SG, Wright B, Nicholson PI, Cooper I, "Robotic path planning for non-destructive testing of complex shaped surfaces," *AIP Conference Proceedings*, Vol. 1650, No. 1, 2015, pp. 1977-1987.
[14] Mineo C, Herbert D, Morozov M, Pierce SG, Nicholson PI, Cooper I, "Robotic non-destructive inspection," Proceedings of 51st Annual Conference of the British Institute of Non-Destructive Testing, 2012.
[15] Secanellas S, et al., "Methodology for the Generation of High-Quality Ultrasonic Images of Complex Geometry Using Industrial Robots," *Sensors*, Vol. 23, No. 5, 2023, 2648.